

Electrochemical Studies on the Recognition of a Ternary Copper Complex to Single-Stranded DNA and Double-Stranded DNA

Feng Gao¹, Qingxiang Wang^{1,*}, Meixia Zheng¹, Shunxing Li², Guoliang Chen¹, Kui Jiao³ and Fei Gao²

¹ Department of Chemistry and Environment Science, Zhangzhou Normal University, Zhangzhou 363000 P. R. China

² Fujian Province University Key Laboratory of Analytical Science, Zhangzhou Normal University, Zhangzhou 363000 P. R. China

³ College of Chemistry and Molecular Engineering, Qingdao University of Science and Technology, Qingdao 266042 P. R. China

*E-mail: axiang236@126.com

Received: 27 January 2011 / Accepted: 5 February 2011 / Published: 1 May 2011

The binding actions of a mixed-ligand copper complex, [Cu(bpy)(MBZ)₂(H₂O)] (bpy = 2, 2'-bipyridine, MBZ = *p*-methylbenzoate) to single-stranded (ss-) DNA and double-stranded (ds-) DNA were comprehensively studied via electrochemical methods in this paper. Cyclic and differential pulse voltammetry carried out in homogeneous solution showed that the copper complex underwent different variation after interaction with dsDNA and ssDNA, showing the different binding mechanism of the copper complex to dsDNA and ssDNA. The determination of the electron-transfer rates (K_s) suggested that the electro-activities of [Cu(bpy)(MBZ)₂(H₂O)]-dsDNA and [Cu(bpy)(MBZ)₂(H₂O)]-ssDNA complexes decreased in different extents compared with the free state of the complex. The thermodynamic binding parameters and kinetic dissociation constants of [Cu(bpy)(MBZ)₂(H₂O)] with dsDNA and ssDNA were also assessed by surface methods. Based on all the results, an intercalative mode of the copper complex to dsDNA and a coordination mode of the copper complex to ssDNA were proposed, which was further testified by the emission experiments.

Keywords: Copper complex, DNA, binding mechanism, fluorescence, electrochemistry

1. INTRODUCTION

DNA (deoxyribonucleic acid) is one of the most important biomacromolecules in the life process since it contains all the genetic information required for cellular function. According to the difference in hierarchy, DNA can be divided into the primary, the second and the tertiary structure and each structure corresponds to its own special biological functions and physicochemical features.

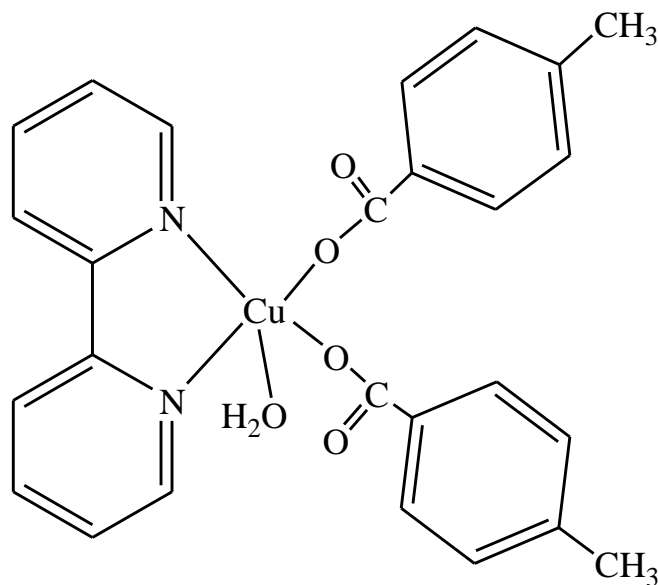
The development of the novel small molecules that have the distinct affinity to DNA with different structures has attracted much attention in the field of DNA researches. These molecules as required can be used as photoactive and electroactive probes of DNA detection [1-3], indicators of DNA hybridization detection [4-6] and chemical nuclease [7]. Currently, according to the structure features of different DNA, many strategies have been applied to design new probes for DNA recognition and analysis. For example, a planar molecule of dipyrido-[3,2-a:2',3'-c]-phenazine (dppz) has often been used as the intercalative ligand in recognition of dsDNA and ssDNA since it can effectively insert into the double helix of dsDNA to achieve stronger specific affinity to dsDNA than to ssDNA [8-10]. Takenaka et al. [11] have synthesized a thread-shape complex that carries an intercalative body of imidazole-substituted naphthalene diimide and two redoxizable ferrocene groups. DNA binding studies showed that the complex can bind to intact calf thymus DNA 4 times stronger than to the denatured DNA, showing good selectivity for ssDNA and dsDNA. However, most of these reported molecules involved complicated preparation process and the binding mechanisms with different DNA have not been fully understood.

The electrochemical methods including pulse polarography, cyclic voltammetry, differential pulse voltammetry, square-wave voltammetry and potentiometric stripping analysis are widely utilized in DNA research today because of their simplicity and accuracy compared with other techniques [12-13]. The detection schemes are mainly based on the redox signaling of the DNA bases [14] or external electroactive small molecules [15, 16]. The traditional electrochemical studies are often performed in homogeneous solution, *i. e.*, both DNA and small molecules are dissolved in solution and then be electrochemically detected.

The limitations of this method such as low sensitivity and the need for large samples of DNA generally cannot meet the needs of DNA studies, especially gene analysis. Recently, surface-based electrochemical method, namely the use of DNA-modified electrodes, are becoming more and more popular as it deserves further investigation regarding the binding activity of molecular analytes on DNA-modified surfaces and the structure-dominated electron transport in the DNA double helix, and these merits are the fundamental and essential perspectives in the development of DNA-based sensing technology [17-20].

Additionally, this method is simple, reliable and require small (microscale) sample, which caters for the demands of gene detection with the development of molecular biology.

In this paper, a facile copper complex with the mixed-ligand of 2, 2'-bipyridine and *p*-methylbenzoate (Chemical structure sees Scheme 1) was synthesized and discrimination to ssDNA and dsDNA were comprehensively investigated by homogeneous solution and DNA-confined surface methods. The data of the electron-transferred rate, binding thermodynamics and dissociation kinetics obtained from electrochemical methods implied that the copper complex likely bound to dsDNA via an intercalative mode and bound to ssDNA via a coordination mode, which was well consistent with the results of the emission experiments. These results suggested this copper complex could be an effective electroactive probe to well recognize ssDNA and dsDNA.



Scheme 1. Chemical structure of [Cu(bpy)(MBZ)₂(H₂O)]

2. EXPERIMENTAL PART

2.1. Reagents and apparatus

Native fish sperm DNA from Beijing Baitai Biochemistry Technology Company (Beijing, China) was used as received. Denatured single-stranded DNA (ssDNA) was produced by thermal denaturation [21]: 0.5 g L⁻¹ dsDNA solution was heated in a water bath at 100 °C for 8 min, and then be rapidly cooled in ice bath. The concentrations of dsDNA in nucleotide phosphate and ssDNA in base were determined spectrophotometrically at 260 nm using the molar extinction coefficient of 6 600 M⁻¹ cm⁻¹ and 8 250 M⁻¹ cm⁻¹, respectively [22]. Methylene blue (MB) was obtained from Shanghai Reagent Company (China). The other reagents such as Tris(hydroxymethyl)aminomethane acetate salt (Tris) base and the materials for synthesizing the copper complex were of analytical grade and purchased commercially. Doubly distilled water was used for preparing all solutions.

Electrochemical experiments were performed on a CHI 832 electrochemical analysis system (CHI Instrument, China) with a three-electrode system consisted of a glassy carbon electrode (GCE, $\Phi = 3$ mm) or DNA modified GCE as the working electrode, a saturated calomel electrode (SCE) as the reference electrode, and a platinum wire as the auxiliary electrode. Fluorescent experiments were measured on an F-4500 Fluorescence Spectrophotometer (Japan).

2.2. Preparation of [Cu(bpy)(MBZ)₂(H₂O)]

The synthesis of the [Cu(bpy)(MBZ)₂(H₂O)] was referred to our previously reported work [23]. Firstly, Cu(MBZ)₂ was obtained by reaction of CuSO₄·5H₂O (1 mmol, 0.25 g) and *p*-methyl benzoate (2 mmol, 0.28 g) in water for 2 h. Then 2, 2'-bipyridine (0.16 g, 1 mmol) dissolved in warm EtOH (50 mL) was added into the above solution and refluxed for 2 h. The resulting solution was

filtered and was left to stand overnight to obtain the blue products. Anal. Calcd. (%) for [Cu(bpy)(MBZ)₂(H₂O)] with half crystal water: C, 60.40; H, 4.87; N, 5.42. Found (%): C, 60.51; H, 4.95; N, 5.34.

2.3. Fluorescent experiments

In the fluorescent experiments, the reaction solution was first prepared by adding the different amount of dsDNA or ssDNA into 20 mM pH 7.1 Tris-HCl buffer containing 10 mM [Cu(bpy)(MBZ)₂(H₂O)] and reacting for 20 min. Before measurement, 20 mM pH 7.1 Tris-HCl buffer was used as the blank to make preliminary adjustments. Then the emission spectra were recorded between 300 nm and 350 nm with the excitation wavelength of 290 nm.

2.4. Electrochemical experiments

The DNA modified electrode was fabricated according to the method described in literature [24]: A freshly polished glassy carbon electrode was firstly electro-oxidized in 0.04 mol/L pH 7.0 phosphate buffer solution for 3 min with a potential +1.7 V. Then the electrode was scanned between -0.3 V and +1.2 V until a constant voltammetric curve was obtained. The pretreated electrode was modified by transferring a droplet of 10 mL of 1 mg/mL dsDNA or ssDNA solution onto its surface, followed by air-drying under 4 °C. It was then soaked in water for more than 3 h and again rinsed with water to remove unadsorbed DNA. Thus, a dsDNA or ssDNA-modified GCE that denoted as dsDNA/GCE or ssDNA/GCE was obtained.

The sensing analysis was performed by immersing ssDNA/GCE or dsDNA/GCE into 20 mM pH 7.1 Tris-HCl buffer solution containing a certain amount of copper complex and electrochemically detected until steady-state voltammetric curves were obtained. The dissociation experiments were carried out by placing dsDNA/GCE or ssDNA/GCE with fully interacted [Cu(bpy)(MBZ)₂(H₂O)] in a cell only containing electrolyte solution (20 mM pH 7.1 Tris-HCl buffer) and electrochemically monitored at regular time intervals until the electrochemical signals become steady.

3. RESULTS AND DISCUSSION

3.1. Electrochemical methods

3.1.1. Homogeneous solution studies

Figure 1 shows the cyclic voltammograms (CV, main panel) and differential pulse voltammograms (DPV, inset) of [Cu(bpy)(MBZ)₂(H₂O)] interaction with the same amount of ssDNA and dsDNA. From CVs, it could be found that [Cu(bpy)(MBZ)₂(H₂O)] exhibited a pair of redox peaks for one electron transfer couple of Cu^{II}/Cu^I at the scan rate of 40 mV/s (curve a). The ratio of oxidation peak current to reduction peak current (I_{pa}/I_{pc}) of 0.5 and the peak-to-peak separation (ΔE_p) of 0.24 V

suggested the characteristic of the electro-transfer process, and this was fairly common for $\text{Cu}^{\text{II}}/\text{Cu}^{\text{I}}$ couple because of the reorganization of the coordination sphere [25].

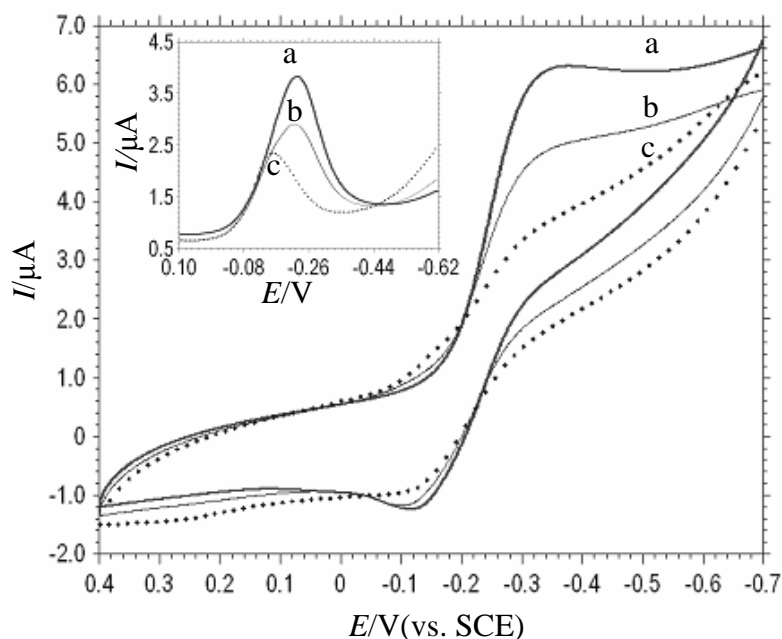


Figure 1. CVs (main panel) and DPVs (inset) of 300 μM $[\text{Cu}(\text{bpy})(\text{MBZ})_2(\text{H}_2\text{O})]$ in the absence (a) and in the presence of 33 μM dsDNA (b) or ssDNA (c) in 20 mM pH 7.1 Tris-HCl. Scan rate for CV: 40 mV s^{-1} . DPV conditions: amplitude, 0.05 V; pulse width, 0.05 s; pulse width, 0.2 s.

After interaction with 33 μM dsDNA, the value of ΔE_p was decreased to 0.18 V (Figure 1b), suggesting that the reversibility of the electron-transfer process of the copper complex was changed better. Moreover, both the oxidation and the reduction peak potentials underwent positive shifts accompanied by the decreases of the redox peak currents. Bard *et al.* [26] had pointed out that the electrochemical potential of the small molecules would shift positively when it intercalated into DNA double helix, and if it bound to DNA by electrostatic interaction, the potential would shift in a negative direction. So, the positive shift of the redox potentials implied that studied copper complex of $[\text{Cu}(\text{bpy})(\text{MBZ})_2(\text{H}_2\text{O})]$ bind to DNA via an intercalation mode.

Interestingly, as compared with the case of dsDNA-binding, the copper complex showed a further decrease in the peak current as well as a further positive shift in the peak potential after interaction with ssDNA (Figure 1c), and this case could be more clearly observed in DPVs as showed in the inset of Figure 1. This phenomenon was conflictive with most of the typical intercalators like echinomycin [27], Nile blue [28] and baicalin [29]. They often showed the stronger association with dsDNA than with ssDNA because they have more binding modes with dsDNA. Obviously, the DNA intercalator presented in this work showed a totally different property compared with above reported molecules. It has been reported that the small molecules can bind to DNA via covalent and non-covalent modes. The covalent interaction often happens for the bases of DNA [30-32]. The non-covalent modes can be further classified into intercalation, groove binding and electrostatic interaction.

Of these, the intercalation and groove binding only take place for dsDNA, while the electrostatic interaction can be happened for both ssDNA and dsDNA as both have the negatively charges on their phosphate backbone. So we thought that the greater affinity of $[\text{Cu}(\text{bpy})(\text{MBZ})_2(\text{H}_2\text{O})]$ with ssDNA than with dsDNA is most likely caused by a specific binding mode of $[\text{Cu}(\text{bpy})(\text{MBZ})_2(\text{H}_2\text{O})]$ with ssDNA.

By comparing the structure features of dsDNA and ssDNA, one can find that bases of ssDNA are often exposed to the external environment, and this greatly enhanced the possibility for ssDNA to interact with other molecules via coordination covalent action as the base contains many electron-rich groups. Many literatures [33, 34] reported that the copper ion has strong coordination with guanine bases. So we deduced that the strong affinity of $[\text{Cu}(\text{bpy})(\text{MBZ})_2(\text{H}_2\text{O})]$ with ssDNA was also likely caused by the coordination interaction of Cu^{II} ion in $[\text{Cu}(\text{bpy})(\text{MBZ})_2(\text{H}_2\text{O})]$ with guanine bases of ssDNA. In order to testify this speculation, a competitive binding assay was carried out via using a phenazine dye of methylene blue (MB) as a model in this work. It has been well known that MB via covalent interaction with guanine affinity with ssDNA than with dsDNA [35-37]. So if both $[\text{Cu}(\text{bpy})(\text{MBZ})_2(\text{H}_2\text{O})]$ and MB can specifically interact with guanine bases, they will be bound to ssDNA competitively.

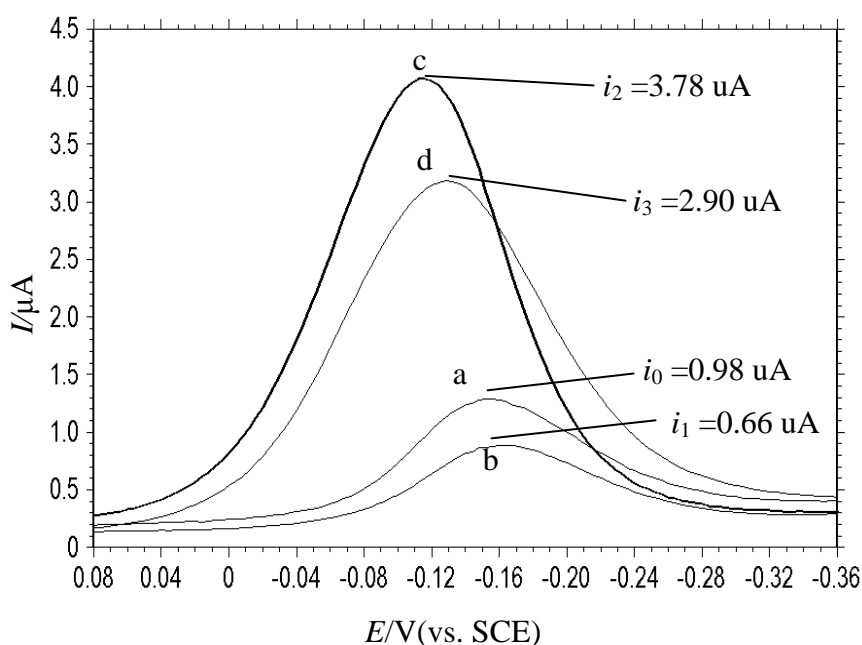


Figure 2. Effect of $[\text{Cu}(\text{bpy})(\text{MBZ})_2(\text{H}_2\text{O})]$ on the DPV of MB-ssDNA system. a. 10 μM MB+500 mM KCl; b a+ 33 μM ssDNA; c. b+ 100 μM $[\text{Cu}(\text{bpy})(\text{MBZ})_2(\text{H}_2\text{O})]$; d. 100 μM $[\text{Cu}(\text{bpy})(\text{MBZ})_2(\text{H}_2\text{O})]$ +33 μM dsDNA+500 mM KCl.

Figure 2 shows the DPVs of competitive interaction of $[\text{Cu}(\text{bpy})(\text{MBZ})_2(\text{H}_2\text{O})]$ and MB with ssDNA. From curve a, the reduction peak current of 10 μM MB was checked to be 0.98 μA (i_0 , curve a). When 33 μM ssDNA was added and then measured after sufficient reaction, the peak current was decreased to 0.66 μA (i_1 , curve b), suggesting the formation of the complex between the MB and

ssDNA. Under the same conditions, 100 μM $[\text{Cu}(\text{bpy})(\text{MBZ})_2(\text{H}_2\text{O})]$ was added, it was found that the peak current increased sharply to 3.78 μA (i_2 , curve c), which was even beyond the peak current of the solution with only MB (i_0 , curve a). Through comparing the reduction peak potentials of MB and $[\text{Cu}(\text{bpy})(\text{MBZ})_2(\text{H}_2\text{O})]$, it could be attributed to the overlap of peaks of MB and $[\text{Cu}(\text{bpy})(\text{MBZ})_2(\text{H}_2\text{O})]$ from the reduction peak of $[\text{Cu}(\text{bpy})(\text{MBZ})_2(\text{H}_2\text{O})]$ as their peak potentials were very close. So, in order to accurately evaluate the effect of $[\text{Cu}(\text{bpy})(\text{MBZ})_2(\text{H}_2\text{O})]$ on the binding of MB to ssDNA, the signal of copper-ssDNA system (i_3 , curve d) should be subtracted. Thus, the result of difference value between i_2 and i_3 , *i. e.*, the “real” peak current of competitive system of $[\text{Cu}(\text{bpy})(\text{MBZ})_2(\text{H}_2\text{O})]$ -MB-ssDNA was obtained to be 0.88 μA , which was significantly larger than the case of MB-ssDNA system (0.66 μA), suggesting that some MB molecules had been released into solution to from MB-ssDNA complex. This just proved that the complex of $[\text{Cu}(\text{bpy})(\text{MBZ})_2(\text{H}_2\text{O})]$ has occupied some sites that had been bound by MB, *i. e.*, the copper complex competitively bound to ssDNA via coordination action.

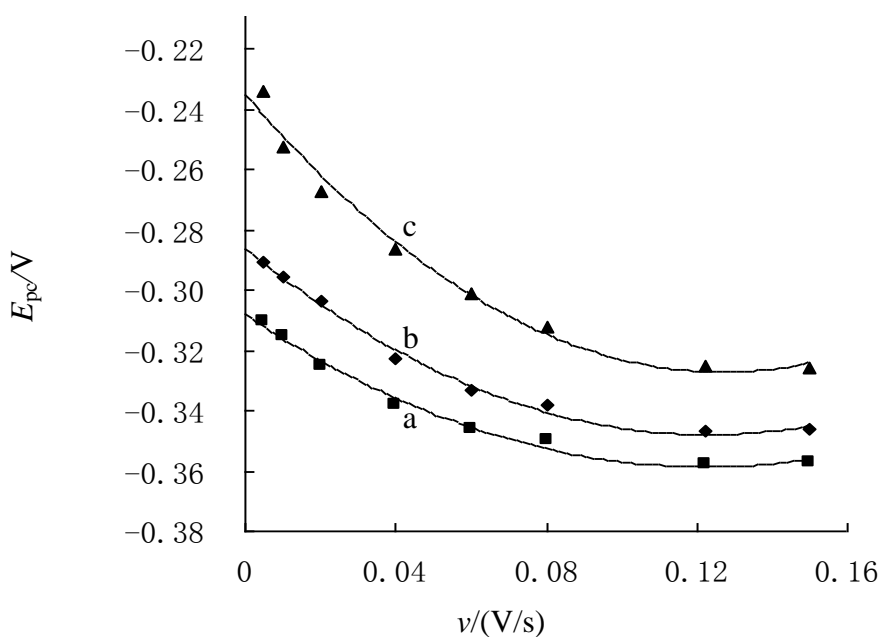


Figure 3. Relationships between reduction peak potentials (E_{pc}) and scan rate (v) of 300 μM $[\text{Cu}(\text{bpy})(\text{MBZ})_2(\text{H}_2\text{O})]$ in the absence (a) or presence of 33 μM dsDNA (b) and ssDNA (c). Supporting electrolyte was 20 mM pH 7.1 Tris-HCl

The change of electron-transferred rate constants (K_s) of electroactive molecules after interaction with DNA was often used to assess the binding natures of small molecules with DNA [38, 39]. In this paper, the K_s values of ssDNA- and dsDNA- bound $[\text{Cu}(\text{bpy})(\text{MBZ})_2(\text{H}_2\text{O})]$ were determined and compared with free $[\text{Cu}(\text{bpy})(\text{MBZ})_2(\text{H}_2\text{O})]$.

Figure 3 showed the relationships of reduction peak potentials (E_{pc}) of $[\text{Cu}(\text{bpy})(\text{MBZ})_2(\text{H}_2\text{O})]$ with scan rate (v) for free (curve a), dsDNA-bound (curve b) and ssDNA-bound (curve c) $[\text{Cu}(\text{bpy})(\text{MBZ})_2(\text{H}_2\text{O})]$. It was found that all the peak potentials for the three systems shifted

negatively with the increase of scan rate (ν). The formal potentials ($E^{0'}$) of free, dsDNA-bound and ssDNA-bound [Cu(bpy)(MBZ)₂(H₂O)] were obtained to be -0.31 V, -0.29 V and -0.24 V, respectively, via prolonging the $E_{pc} \sim \nu$ curves to y axis. Moreover, for each system, the reduction peak potentials showed good linear relationships with the logarithm of scan rate ($\ln \nu$) (Figure 4).

Thus, the K_s values were calculated to be 0.35 s⁻¹, 0.28 s⁻¹ and 0.20 s⁻¹, respectively for free, dsDNA-bound and ssDNA-bound [Cu(bpy)(MBZ)₂(H₂O)] according to the linear regression equation of $E_{pc} \sim \ln \nu$ and the following Laviron's equation [40]:

$$E_{pc} = E^{0'} + RT/(anF) \ln RTK_s/(anF) - RT/(anF) \ln \nu \quad (1)$$

Where α was the electron transfer coefficient, F the Faraday constant (96487 coulombs), R the universal gas constant (8.314 J K⁻¹ mol⁻¹), T the Kelvin temperature (K), and n the number of electron-transferred.

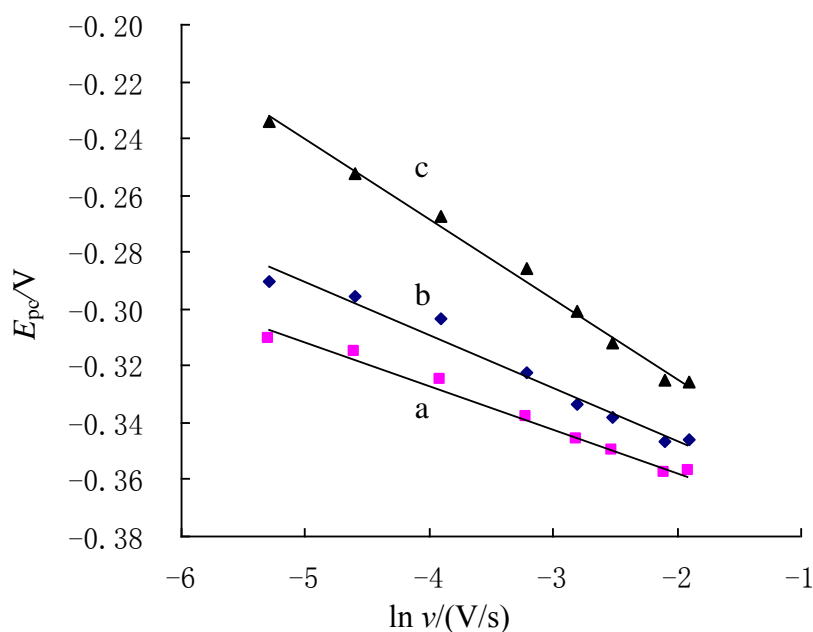


Figure 4. Relationships between E_{pc} and the logarithm of scan rate ($\ln \nu$) of Cu(bpy)(MB)₂ in the absence (a) and presence of dsDNA (b) or ssDNA (c). Conditions were the same with Figure 3.

This was to say, after interaction with dsDNA and ssDNA, the electron-transferred rate (K_s) fallen to the 80% and 57% of the free form, respectively. The lower K_s value of ssDNA-[Cu(bpy)(MBZ)₂(H₂O)] than that of dsDNA-[Cu(bpy)(MBZ)₂(H₂O)], from another point of view, suggested that the electrochemical activity of ssDNA-[Cu(bpy)(MBZ)₂(H₂O)] was much weaker than that of dsDNA-[Cu(bpy)(MBZ)₂(H₂O)] complex, and this likely was another reason for the different redox response of [Cu(bpy)(MBZ)₂(H₂O)] after interaction with dsDNA and ssDNA.

3.1.2. Surface-based electrochemical studies

The recognition properties of [Cu(bpy)(MBZ)₂(H₂O)] to ssDNA and dsDNA were also determined by electrochemical sensing method in this paper. Figure 5 shows the CVs of

[Cu(bpy)(MBZ)₂(H₂O)] at bare GCE (curve a), ssDNA/GCE (curve b) and dsDNA/GCE (curve c), respectively. It was clear that the CV curves of [Cu(bpy)(MBZ)₂(H₂O)] at ssDNA/GCE and dsDNA/GCE were obviously different with that at bare GCE. On dsDNA/GCE, both the reduction and oxidation peaks underwent positive shifts, suggesting that [Cu(bpy)(MBZ)₂(H₂O)] still interacted intercalatively with dsDNA at GCE surface [17]. The difference value of +30 mV in $E_{1/2}$ (average value of oxidation and reduction peak potentials) suggested that the reduced form of the complex, [Cu^I(bpy)(MBZ)₂(H₂O)] interacted with dsDNA at the electrode surface more strongly (3 times) than the oxidized form, [Cu^{II}(bpy)(MBZ)₂(H₂O)] according to the following equation [17]:

$$\Delta E_{1/2} = E_{1/2,\text{surf}} - E_{1/2,\text{sol}} = -RT/(nF) \ln(K_{\text{Ox}}/K_{\text{Red}}) \quad (2)$$

In the equation, $E_{1/2,\text{surf}}$ and $E_{1/2,\text{sol}}$ represented the average value of oxidation and reduction peak potentials of the redox species determined at the electrode surface and in solution, respectively; K_{Ox} and K_{Red} were the surface binding constants for the oxidized and reduced forms of the redox species to dsDNA, respectively.

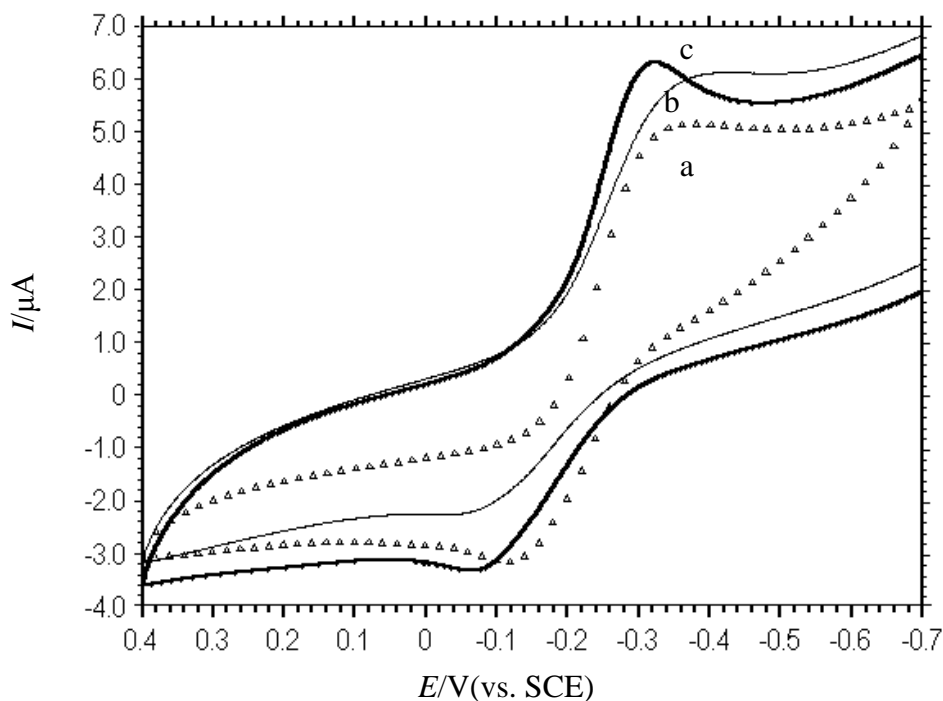


Figure 5. CVs of 300 μM [Cu(bpy)(MBZ)₂(H₂O)] in 20 mM pH 7.1 Tris-HCl buffer at bare GCE (a), ssDNA/GCE (b) and dsDNA/GCE (c). Scan rate = 40 mV s^{-1} .

Thus, from the result, it could be obtained that the reduction form of the complex showed a stronger affinity with dsDNA, which was well consistent with a typical intercalative binding mode [17]. Additionally, the value of $I_{\text{pa}}/I_{\text{pc}}$ at dsDNA/GCE was changed to be about one unit with a small decrease of ΔE_{p} , suggesting that the electron-transfer reversibility of the complex was changed better as compared with the bare electrode.

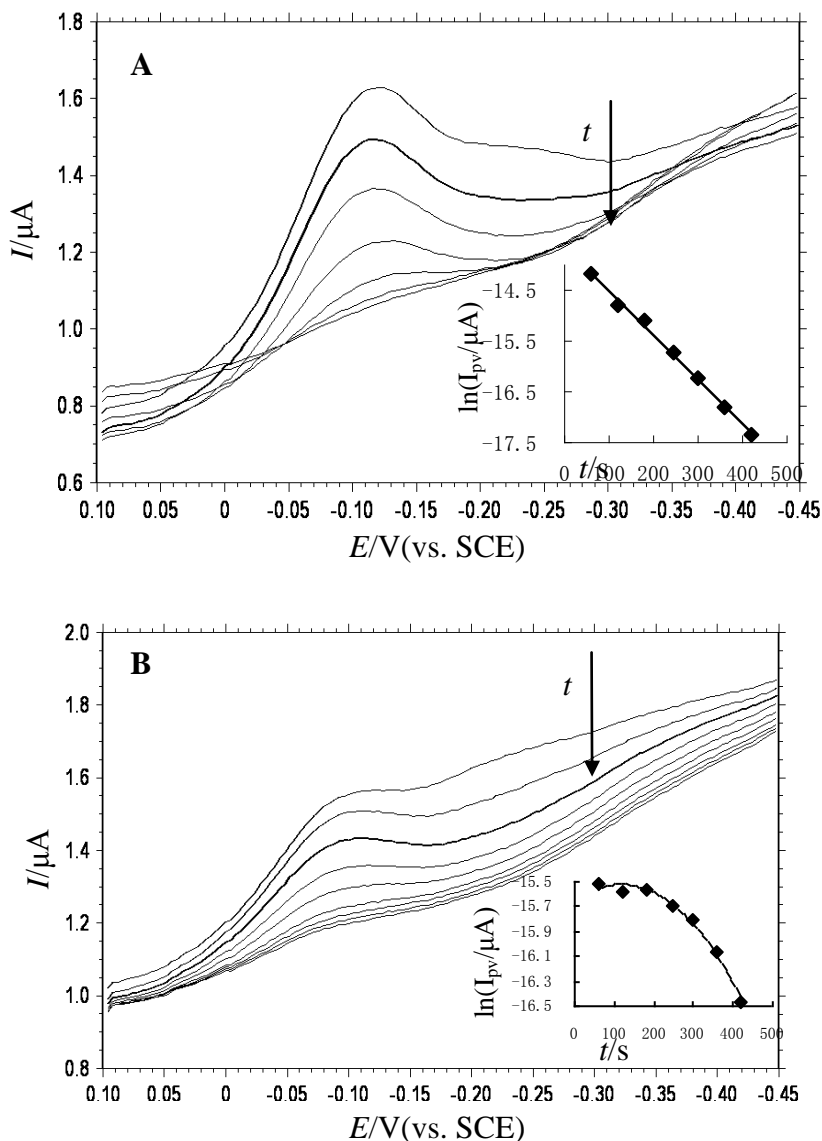
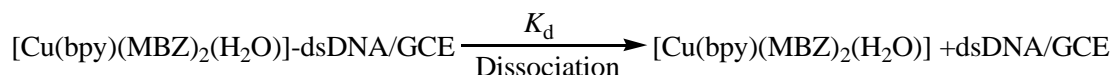


Figure 6. Time-dependent DPVs obtained in 20 mM pH 7.1 Tris-HCl at dsDNA/GCE (A) and ssDNA/GCE (B) after immersing the modified electrodes into 300 μM $[\text{Cu}(\text{bpy})(\text{MBZ})_2(\text{H}_2\text{O})]$ for equilibrium. Insets: plots of $\ln I_{\text{pc}}$ versus dissociation time (t) obtained from dsDNA/GCE (A) and ssDNA/GCE (B)

However, at ssDNA/GCE, the redox peak currents of $[\text{Cu}(\text{bpy})(\text{MBZ})_2(\text{H}_2\text{O})]$ decreased obviously coupled with an increase of peak-to-peak separation (ΔE_{p}) (Figure 5b), which suggested that the electroactivity and the electron-transfer kinetics of the complex were both suppressed at ssDNA/GCE. With the consideration of the changes of the electron transfer rate (K_{s}) obtained from previous solution-based studies, the decrease of peak currents could be assigned to the decrease of electrochemical activity of the copper complex after coordination with ssDNA at GCE surface. Furthermore, the coordination action of $[\text{Cu}(\text{bpy})(\text{MBZ})_2(\text{H}_2\text{O})]$ with ssDNA inhibited the electron-transfer kinetic of the complex as ssDNA was not a perfect conductor for electron exchange [41].

The dissociation process of $[\text{Cu}(\text{bpy})(\text{MBZ})_2(\text{H}_2\text{O})]$ from dsDNA/GCE and ssDNA/GCE were further carried out to investigate the different kinetic binding action of $[\text{Cu}(\text{bpy})(\text{MBZ})_2(\text{H}_2\text{O})]$ to

dsDNA and ssDNA. Figure 6A was the time-dependent DPVs of the copper complex obtained in the background solution at the pre-concentrated dsDNA/GCE. It can be seen that the reduction peak grew lower and lower, and essentially disappeared after 15 min owing to the complete dissociation of [Cu(bpy)(MBZ)₂(H₂O)] from dsDNA/GCE into the background solution. The logarithm values of the reduction peak currents (ln I_{pc}) depended linearly on the dissociation time (t) as showed in the inset of Figure 6A, illustrating that the dissociation process was well obeyed the first-order kinetics according to the following model [17]:



Thus, the dissociation rate constant (K_d) could be determined to be $8.9 \times 10^{-3} \text{ s}^{-1}$ according to the first order kinetic equation:

$$\ln I_{pc} = -K_d t + \text{“constant”} \quad (3)$$

While, on ssDNA/GCE, the peak currents of the absorbed [Cu(bpy)(MBZ)₂(H₂O)] were very stable within 200 s (Figure 6B), suggesting that the bound copper complex was hard to dissociate from ssDNA/GCE at the incipient stage. When the dissociation time was upon 200 s, the peak was attenuated slowly and, ln I_p didn't obeyed a linear relationship with t during the whole dissociation process as showed in the inset of Figure 6B, suggesting that the dissociation of the copper complex from ssDNA/GCE didn't measure up with the first-order kinetics. As discussed above, the copper complex bound to ssDNA via coordination action, and this kind of action should be much stronger than the non-covalent mode of intercalation, which might be the critical reason to induce the different dissociation process at the two modified electrodes. This also indicated that this copper complex had different binding action with ssDNA and dsDNA.

3.2. Fluorescent experiments

The different binding actions of the copper complex with ssDNA and dsDNA were also investigated by fluorescent spectra studies. It has been well known that the different binding modes of small molecules with DNA usually resulted in the different variation of the characteristic spectrum of the small molecules [42-44]. Figure 7 shows the emission spectra of [Cu(bpy)(MBZ)₂(H₂O)] after interaction with different concentrations of dsDNA (A) and ssDNA (B). As seen, the copper complex showed relatively weak emission spectra at 330 nm in Tris-HCl buffer (curve a. in Figure 7). Upon titrating increasing concentrations of dsDNA into the copper solution, the fluorescence intensity of the complex was enhanced gradually (curve b~d in Figure 7A). According to the reported “DNA molecular light switches” phenomenon, the enhanced effect could be ascribed to the protection of the coordinated pyridine nitrogen atoms from solvent water as the bipyridine ligand in [Cu(bpy)(MBZ)₂(H₂O)] intercalated between the adjacent base pairs of dsDNA [45]. From this assay, the copper complex into the base pairs of dsDNA could be further identified. However, the interaction

of $[\text{Cu}(\text{bpy})(\text{MBZ})_2(\text{H}_2\text{O})]$ with ssDNA showed a totally contrary change of the fluorescent intensity. As showed in Figure 6B, the emission intensity of the $[\text{Cu}(\text{bpy})(\text{MBZ})_2(\text{H}_2\text{O})]$ decreased gradually after interaction with increasing amount of ssDNA (curve b~d in Figure 7B). This quenching effect was commonly related the direct photoelectron-transfer process of the bases of DNA to the excited complex [46], *i. e.*, the coordination of copper(II) ions with the bases of ssDNA. So, this different variation of the emission spectra of $[\text{Cu}(\text{bpy})(\text{MBZ})_2(\text{H}_2\text{O})]$ after interaction with ssDNA and dsDNA further implied that the copper complex bound to ssDNA and dsDNA via different modes, *i. e.*, the coordinative and intercalative modes, respectively, and this result was well in agreement with the electrochemical experiments. On the other hand, it could be obtained that this complex could be applied as an effective electroactive and photoactive probe to recognize ssDNA and dsDNA.

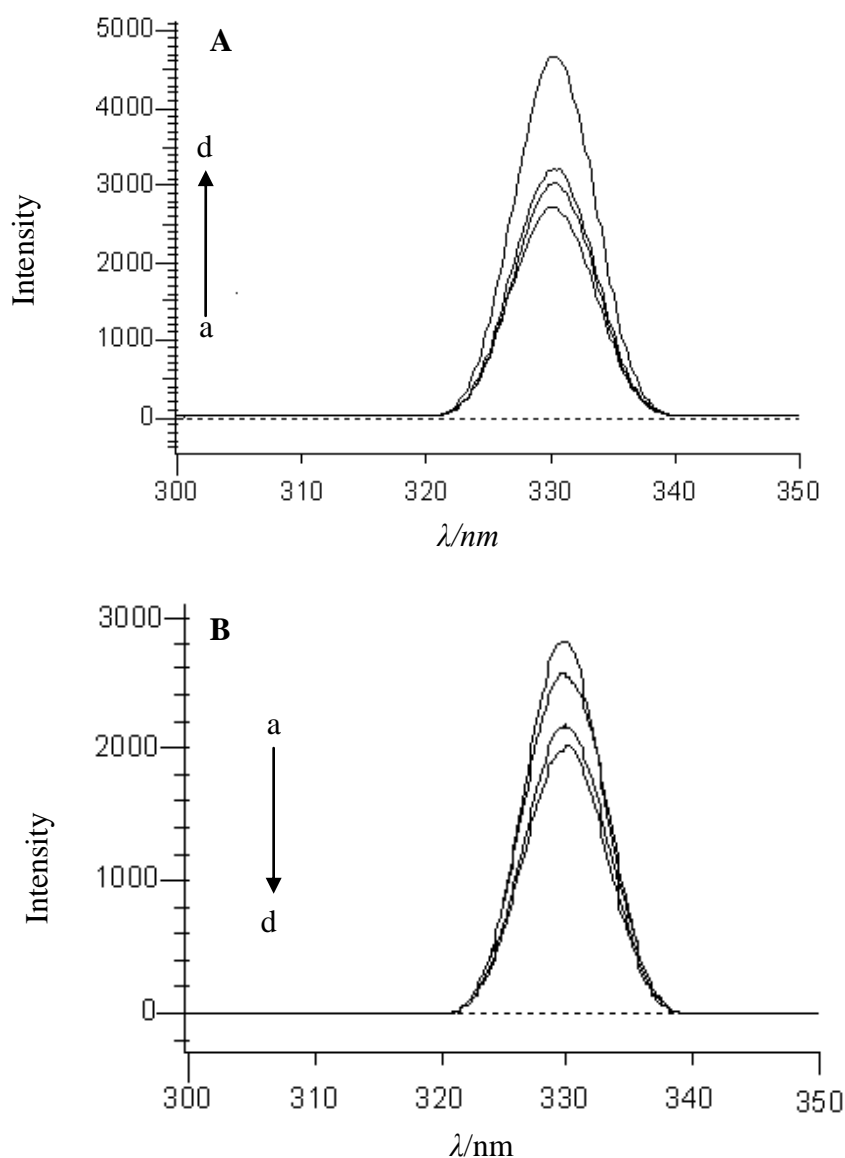


Figure 7. Emission spectra of 10 mM $[\text{Cu}(\text{bpy})(\text{MBZ})_2(\text{H}_2\text{O})]$ in 20 mM pH 7.1 Tris-HCl buffer with 500 mM KCl in the presence of 0 (a), 3.3 (b), 9.9 (c) and 16.5 (d) μM dsDNA (A) and ssDNA (B).

4. CONCLUSIONS

The screening and application of novel electroactive molecules for probing DNA structure and function were of very promising in DNA analysis. In the present research, the different binding action of an electro-neutral copper complex to ssDNA and dsDNA were systematically studied by surface- and solution- electrochemical methods. Based on the different variation of electrochemical signals of the copper complex after interaction with ssDNA and dsDNA, it was obtained that the copper complex could be used as an effective discriminator for primary and second structure of DNA. According to the results of the direct interaction and the indirect competitive binding with EB, an intercalative mode with dsDNA and a coordinative action with ssDNA for the complex were proposed, and these conclusions were finally testified by the emission spectra experiments.

ACKNOWLEDGMENTS

The work is supported by the National Natural Science Foundation of China (Nos. 20805041, 20977074), Training Programme Foundation for Excellent Youth Researching Talents of Fujian's Universities (No. JA10201) and Major Program of Enterprise-College-Research of Fujian's Science & Technology Department (No. 2010H6029).

Reference

1. S. Delaney, M. Pascaly, P.K. Bhattacharya, K. Han and J.K. Barton, *Inorg. Chem.*, 41 (2002) 1966.
2. Q.X. Wang, K. Jiao, W. Sun, F.F. Jian and X. Hu, *Euro. J. Inorg. Chem.*, 2006 (2006) 1838.
3. H. Ilkhani, M.R. Ganjali, M. Arvand and P. Norouzi, *Int. J. Electrochem. Sci.*, 5 (2010) 168.
4. C. Ding, F. Zhao, M. Zhang and S. Zhang, *Bioelectrochemistry*, 72 (2008) 28.
5. H.Y. Shen, H.M. Zheng, N. Zhu, Y.Q. Liu, J. Gao, Jia Li, *Int. J. Electrochem. Sci.*, 5(2010)1587.
6. E.G. Hvastkovs and D.A. Buttry, *Anal. Chem.*, 79 (2007) 6922.
7. D. Lahiri, R. Majumdar, A.K. Patra and A.R. Chakravarty, *J. Chem. Sci.*, 122 (2010) 321.
8. C.G. Coates, J.J. McGarvey, P.L. Callaghan, M. Coletti and J.G. Hamilton, *J. Phys. Chem. B*, 105 (2001) 730.
9. K.K.W. Lo, C.K. Chung and N. Zhu, *Chem. Eur. J.*, 12 (2006) 1500.
10. K. Maruyama, Y. Mishima, K. Minagawa and J. Motonaka, *Anal. Chem.*, 74 (2002) 3698.
11. S. Takenaka, K. Yamashita, M. Takagi, Y. Uto and H. Kondo, *Anal. Chem.*, 72 (2000) 1334.
12. S.M. Wang, W.Y. Su and S.H. Cheng, *Int. J. Electrochem. Sci.*, 5 (2010) 1649.
13. M. Ravera, S. Baracco, C. Cassino, D. Colangelo, G. Bagni, G. Sava and D. Osella, *J. Inorg. Biochem.*, 98 (2004) 984.
14. H. Karadeniz, A. Erdem and A. Caliskan, *Electroanalysis* 20 (2008) 1932.
15. G. Ziyatdinova, J. Galandova, J. Labuda, *Int. J. Electrochem. Sci.*, 3 (2008) 223.
16. A.Liu and J. Anzai, *Anal. Chem.* 76 (2004) 2975.
17. W. Sun, M. Yang and K. Jiao, *Int. J. Electrochem. Sci.*, 2 (2007) 93.
18. F. Wang, Y. Wu, J. Liu and B. Ye, *Electrochim. Acta*, 54 (2009) 1408
19. J.B. Raouf, M.S. Hejazi, R. Ojani, E.H. Asl, *Int. J. Electrochem. Sci.*, 4 (2009) 1436.
20. Q.X. Wang, F. Gao, K. Jiao, *Electroanalysis*, 20 (2008) 2096.
21. D.W. Pang and H.D. Abruna, *Anal. Chem.*, 70 (1998) 3162.
22. M.E. Reichman, S.A. Rice, C.A. Thomas and P. Doty, *J. Am. Chem. Soc.*, 76 (1954) 3047.
23. F.Q. Liu, Q.X. Wang, K. Jiao, F.F. Jian, G.Y. Liu and R.X. Li, *Inorg. Chim. Acta.*, 359 (2006) 1524.

24. X. Hu, K. Jiao, W. Sun and J.Y. You, *Electroanalysis*, 18 (2006) 613.
25. M. Palaniandavar, T. Pandiyan, M. Lakshminarayanan and H. Manohar, *J. Chem. Soc. Dalton. Trans.*, (1995) 455.
26. M.T. Carter, M. Rodriguez and A.J. Bard, *J. Am. Chem. Soc.*, 111 (1989) 8901.
27. F. Jelen, A. Erdem and E. Palecek, *Bioelectrochemistry*, 55 (2005) 165.
28. H. Ju, Y. Ye and Y. Zhu, *Electrochim. Acta*, 50 (2005) 1361.
29. Y. Hashimoto and K. Shudo, *Environ. Health Persp.*, 62 (1985) 215.
30. L. A. Margulis, V. Ibanez and N. E. Geacintov, *Chem. Res. Toxicol.*, 6 (1993) 59.
31. M.H. David-Cordonnier, W. Laine, A. Lansiaux, F. Rosu, P. Colson, E. de Pauw, S. Michel, F. Tillequin, M. Koch, J.A. Hickman, A. Pierre and C. Bailly, *Mol. Cancer Ther.*, 2005 4 (2005) 71.
32. F. Secco, M. Venturini, M. Lopez, P. Perez, R. Prado and F. Sanchez, *Phys. Chem. Chem. Phys.*, 3 (2001) 4412.
33. L. Li, N.N. Murthy, J. Telser, L.N. Zakharov, G.P. Yap, A.L. Rheingold, K.D. Karlin and S.E. Rokita, *Inorg. Chem.*, 45 (2006) 7144.
34. X.H. Lin, Wu P. Wu, W. Chen, Y.F. Zhang and X.H. Xia, *Talanta*, 72 (2007) 468.
35. A.Tani, A.J. Thomson and J.N. Butt, *Analyst*, 126 (2001) 1756.
36. P. Kara, K. Kerman, D. Ozkan, B. Meric, A. Erdem, Z. Ozkan and M. Ozsoz, *Electrochem. Commun.*, 4 (2002) 705.
37. Q.X. Wang, K. Jiao, F.Q. Liu, X.L. Yuan and W. Sun, *J. Biochem. Biophys. Methods*, 70 (2007) 427.
38. J. Li, G. Cheng and S. Dong, *Electroanal.*, 9 (2005) 834.
39. E. Laviron, *J. Electroanal. Chem.*, 101 (1979) 19.
40. T. Liu and J.K. Barton, *J. Am. Chem. Soc.*, 127 (2005) 10160.
41. C.V. Kumar and E.H. Asuncion, *J. Am. Chem. Soc.*, 115 (1993) 8541.
42. L. Jia, P. Jiang, J. Xu, Z. Hao, X. Xu, L. Chen, J. Wu, N. Tang, Q. Wang and J.J. Vittal, *Inorg. Chim. Acta.*, 363 (2010) 855.
43. M. Khorasani-Motlagh, M. Noroozifar and S. Mirkazehi-Rigi, *Spectrochim Acta A*, 75 (2010) 598.
44. A.E. Friedman, J.C. Chambron, J.P. Sauvage, N.J. Turro and J.K. Barton, *J. Am. Chem. Soc.*, 112 (1990) 4960.
45. J.M. Kelly, D.J. McConnell, C. OhUigin, A.B. Tossi and A. Kirsch-De Mesmaeker, A. Masschelein, J. Nasielski, *J. Chem. Soc. Chem. Comm.*, 24 (1987) 1821.